



Ab initio prediction of environmental embrittlement at a crack tip in aluminum

R. J. Zamora,¹ A. K. Nair,¹ R. G. Hennig,² and D. H. Warner¹

¹*School of Civil and Environmental Engineering, Cornell University, Ithaca, New York 14853, USA*

²*Department of Materials Science and Engineering, Cornell University, Ithaca, New York 14853, USA*

(Received 20 April 2012; revised manuscript received 1 June 2012; published 2 August 2012)

We report on *ab initio* predictions of environmental embrittlement in aluminum. We have used an atomistic-continuum multiscale framework to simulate the behavior of a loaded crack tip in the presence of oxygen and hydrogen. The multiscale simulations and subsequent analysis suggest that electronegative surface impurities can inhibit dislocation nucleation from a loaded crack tip, thus raising the likelihood for incremental brittle crack growth to occur during near-threshold fatigue. The metal-impurity bonding characteristics have been analyzed using a Bader charge transfer approximation, and the effect of this bond on the theoretical slip distribution has been investigated using a continuum Peierls model. The Peierls model, which is a function of the position dependent stacking fault energy along the slip plane, was used to estimate the effects of several common environmental impurities.

DOI: [10.1103/PhysRevB.86.060101](https://doi.org/10.1103/PhysRevB.86.060101)

PACS number(s): 62.20.mm, 81.40.Np, 31.15.A–

The presence of environmental impurities is known to promote crack growth in a variety of technologically important materials.¹ For example, when aluminum is subjected to cyclical loading in a controlled atmosphere, a rise in humidity will accelerate the crack growth process and lower the threshold load required for fatigue to occur.² To explain the origin of this environmental embrittlement phenomenon, a wide variety of theoretical mechanisms have been hypothesized from a top-down approach, using the wealth of experimental data and microscopy presented in the literature.^{3,4}

It is now possible to use atomistic modeling capabilities to investigate classical embrittlement mechanisms from a bottom-up approach.^{5–8} Such models can be used to observe bond rupture as it occurs, thus potentially illuminating chemomechanical details. In the past, atomistic modeling was limited when used to investigate fracture processes, because it was a significant challenge to enforce accurate interatomic force calculations while considering long range elastic interactions. Fortunately, growing supercomputing resources and advances in concurrent multiscale modeling techniques^{9–12} are now beginning to make accurate atomic-scale simulations of crack growth more feasible.

In this spirit, the current work provides a direct *ab initio* glimpse into the chemomechanical interactions that occur at a metal crack tip in the presence of environmental surface impurities. The crack tip simulations were made possible by combining the quantum-mechanical coupled atomistic discrete dislocation (QM-CADD) framework and the NASA Pleiades supercomputer.

We have examined three distinct crack tip configurations: (1) a crack tip with no impurities, (2) a crack tip with a single hydrogen impurity, and (3) a crack tip with a single oxygen impurity. Each simulation was initialized at a stable stress intensity factor (K_I), and the load was ramped through a succession of increments until equilibrium could no longer be reached without the nucleation of a partial dislocation. Here we use the term K_{IN} to define the critical stress intensity factor required for nucleation to occur. To estimate the relative charge transfer induced by each impurity, a Bader analysis was performed on the electron charge density solution for each configuration at

the same load. The mechanical effect of the perturbed charge distribution was determined by calculating the energetic resistance to shear along each slip plane. This energy functional was used within a continuum Peierls model to arrive at a critical load prediction. A consistent strengthening effect was observed for all crack tip simulations in the presence of oxygen and hydrogen. Although the continuum model yields a similar strengthening effect for any electronegative surface impurity, the results of QM-CADD suggest that a unique embrittlement mechanism takes place in the presence of hydrogen.

The QM-CADD atomistic-continuum framework is a reliable way to investigate crack tip mechanisms involving complex metal-impurity bonding. The multiscale framework allows for the computation of high fidelity interatomic forces by requiring that only the small nonlinear region of material surrounding the crack tip is modeled atomistically. Here we use Kohn-Sham density functional theory (KS-DFT) in the atomistic region and linear elastic finite elements in the surrounding region (see Fig. 1). The two regions are coupled by an iterative force balance approach, and the relevant coupling errors have been minimized by the methods discussed in Refs. 12 and 13. Broadly, one can consider the QM-CADD approach to be identical to its ancestor, developed by Shilkrot *et al.*,¹⁴ but with the original empirical potential driven interatomic force calculation replaced by a quantum-mechanical Hellman-Feynman force calculation.¹⁵

All simulations were built upon the ductile aluminum crack tip geometry depicted in Fig. 1. In this configuration, we use a $20\,000\text{ \AA} \times 20\,000\text{ \AA}$ continuum domain with a crack, terminating at a $58\text{ \AA} \times 55\text{ \AA}$ atomistic region. The crack was created by removing three (111) planes from a pristine material, preventing the crack from closing at small loads. The resulting atomistic region consisted of a total of 442 aluminum atoms, of which 326 were distributed in the pad region in order to buffer the crack tip from possible vacuum effects.

All interatomic force calculations were performed within the Vienna *ab initio* simulation package (VASP), in which ultrasoft pseudopotentials and a plane wave basis set were used to solve the equations of KS-DFT.¹⁶ Within VASP, the local density approximation (LDA) was used, along with a

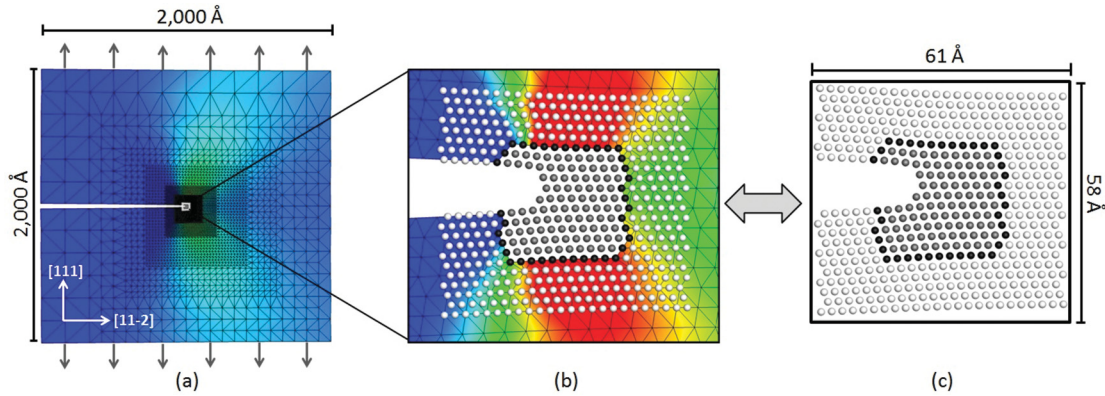


FIG. 1. (Color online) QM-CADD simulation setup for studying crack tip dislocation nucleation: (a) Overall geometry with color contours showing uniaxial strain in the vertical direction; (b) zoomed view of the crack tip region, showing the inner ions (gray), the interface ions (black), and the pad ions (white); and (c) the Kohn-Sham DFT simulation cell consisting of the inner, interface, and pad ions surrounded by a small vacuum in a periodic unit cell. The three-dimensional atomic structure is projected onto the two-dimensional (2D) plane for visual clarity.

$1 \times 1 \times 8$ k -point mesh, a Methfessel-Paxton smearing of 1 eV,¹⁷ and a plane wave cutoff of 250 eV. All atomistic visualization was performed in VESTA.¹⁸

A meaningful atomistic discretization of the continuous charge density field was obtained by dividing space into regions using a Bader surface designed to satisfy the relationship $\nabla \rho(\vec{r}_s) \cdot \hat{n}(\vec{r}_s) = 0$, where \vec{r}_s is a point on the Bader surface and $\hat{n}(\vec{r}_s)$ is the normal vector to the surface at that point.

Using the QM-CADD framework to model the pure aluminum crack tip configuration, the critical load required for nucleation was found to occur at a stress intensity of $0.245 \text{ eV}/\text{\AA}^{2.5}$. At this load there was a clear relative motion of atoms across the $(11\bar{1})$ plane in the $[112]$ direction, indicative of the nucleation of a partial dislocation from the free surface. As expected for a ductile metal, plasticity occurred on the most highly sheared slip plane without any sign of incipient cleavage or crack advancement.

The presence of oxygen and hydrogen at the surface of the crack tip was observed to increase the critical nucleation load. While oxygen resulted in dislocation nucleation on the same slip plane as in the pure aluminum case, hydrogen resulted in dislocation nucleation on a different slip plane (Fig. 2). More specifically, the presence of hydrogen led to crack advancement by a single atomic spacing and dislocation nucleation on the newly exposed slip plane. Thus, both impurity elements were observed to inhibit crack tip plasticity, while hydrogen qualitatively changed the response of the crack tip in that it led to incremental crack advancement.

Figure 3 shows the KS-DFT electron charge density solutions calculated during QM-CADD simulations at a stable load of $K_I = 0.235 \text{ eV}/\text{\AA}^{2.5}$. The results of the Bader analysis¹⁹ of the valence charge density in Table I show that oxygen and hydrogen both form an ionic bond with the nearest aluminum atom, leading to a filled valence shell, as expected from electronegativity differences. The charge transfer at the impurity site clearly influences the interatomic bonding across the slip plane, which is ultimately the source of the higher critical nucleation loads observed in the mechanical simulations.

To better understand this process, we analyzed the crack tip dislocation nucleation mechanism using an atomistically

informed Peierls continuum model.²⁰ The Peierls model simplifies the dislocation nucleation process to a continuum

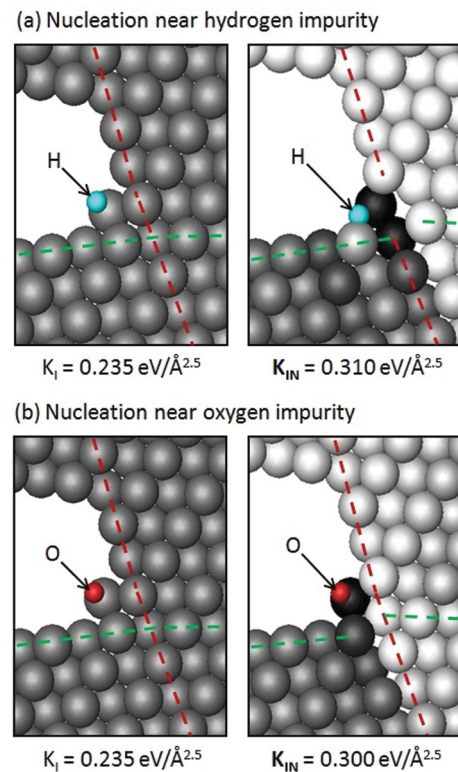


FIG. 2. (Color online) Dislocation nucleation process in the presence of environmental impurity atoms: (a) Hydrogen causes nucleation to occur at a stress intensity load of $0.310 \text{ eV}/\text{\AA}^{2.5}$. (b) Oxygen causes nucleation to occur at a stress intensity load of $0.300 \text{ eV}/\text{\AA}^{2.5}$. Equilibrium crack tip configurations for both impurities are shown at $K_I = 0.235 \text{ eV}/\text{\AA}^{2.5}$, where both configurations are stable and dislocation free. In both nucleated configurations, aluminum atoms are shaded by their motion in the slip plane direction relative to the previous load step. It is clear from these images and the fiducial markers that hydrogen causes slip to occur on a different slip plane than oxygen.

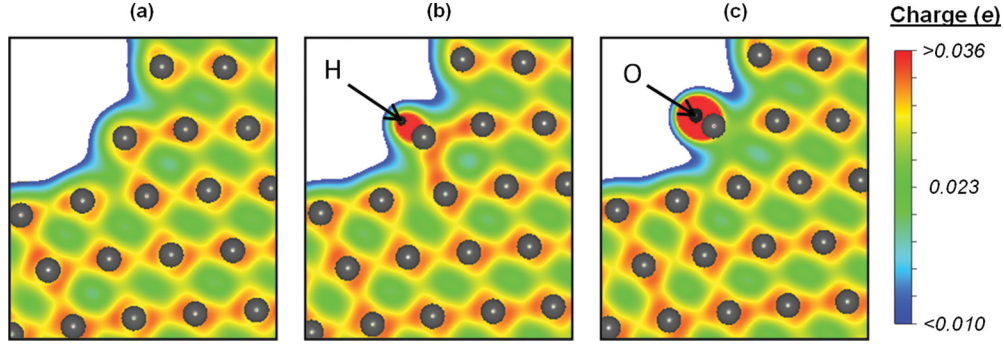


FIG. 3. (Color online) Contour images of the valence electron charge density field for each of the three crack tip configurations at $K_I = 0.235 \text{ eV}/\text{\AA}^{2.5}$. Atomic positions are projected onto the 2D contour image, which was taken on the plane halfway between atoms in the $[\bar{1}10]$ direction in all three plots: (a) Pure aluminum crack tip configuration; (b) and (c) the same configuration with hydrogen and oxygen added, respectively. Although both impurities have an effect on the charge transfer induced near the slip plane, the resulting charge density fields are clearly different. All contour units are in elementary electron charge (e).

mechanics problem involving a loaded linear elastic body with an embedded slip plane capable of producing a shear displacement jump in the material. Accordingly the energy of the model system is then a function of the elastic strain energy stored in the bulk material and the nonlinear localized energy penalty associated with slip on the slip plane, i.e., the stacking fault energy curve. At low loads, a unique slip distribution exists that corresponds to the unstable equilibrium state of the system (the barrier state for dislocation nucleation). The minimum load at which this barrier state ceases to exist represents the critical load for dislocation nucleation to occur instantaneously.

Traditionally, the stacking fault energy curve is often assumed to be independent of position.^{20,21,25} This effectively corresponds to ignoring the influence of the free surface on interatomic bonding. Alternatively, in this analysis we computed the stacking fault energy curve using KS-DFT as a function of both plastic slip and distance along the slip plane from the crack surface r . This was accomplished by rigidly shearing the crack tip configuration used in the

QM-CADD simulation along the slip plane and integrating Hellman-Feynman forces to define the stacking fault energy curve as a function of r .

The energy balance relationship used in the continuum Peierls dislocation model is

$$U[\delta(r)] = U_o + \int_0^\infty \Phi[\delta(r), r] dr + \frac{1}{2} \int_0^\infty s[\delta(r)] \delta(r) dr - \int_0^\infty \sigma_{r\theta}(r) \delta(r) dr. \quad (1)$$

In this relationship U_o is the energy of the loaded elastic system in which the slip distribution $\delta(r)$ is confined to be zero along the slip plane. $\Phi[\delta(r), r]$ is the local nonlinear component of the energy penalty associated with slip and is derived from the stacking fault energy curves,²⁰ e.g., Fig. 4. $s[\delta(r)]$ is the stress distribution on the slip plane created by the slip distribution,

$$s[\delta(r)] = \frac{\mu}{2\pi(1-\nu)} \int_0^\infty \sqrt{\frac{\xi}{r}} \frac{d\delta(\xi)/d\xi}{r-\xi} d\xi. \quad (2)$$

The remaining term in Eq. (1) represents the elastic work done by the slip distribution acting against the applied load $\sigma_{r\theta}(r, \rho, K_I, \theta)$. The relevant form of the applied load, as derived in Ref. 26, is dependent upon the radius of curvature of the crack tip ρ , the applied stress intensity factor K_I , and the orientation of the slip plane θ . In the calculations conducted here, the shear modulus (μ) was taken as 46.9 GPa and the crack tip radius as 2.0 \AA . The critical nucleation load was obtained by incrementing the applied stress intensity factor until the slip distribution corresponding to the local minimum of Eq. (1) failed to converge. For each load increment the equilibrium slip distribution was found numerically using a standard Newton-Raphson approach.

The stacking fault energies were found to be significantly influenced by the free surface to a depth of 1 nm into the material, and beyond this scale the energies approached that of the bulk. The influence of surface impurities on the stacking fault energy was found to have a similar range (Fig. 4). Considering that the critical state for partial dislocation

TABLE I. Results of the Bader charge transfer analysis, QM-CADD simulations, and continuum model simulations. Charge units are displayed as the negative electron charge ($-e$), and K_{IN} units are in $\text{eV}/\text{\AA}^{2.5}$. The ‘‘impurity effect’’ was calculated as the percent change in K_{IN} with respect to the pure aluminum simulation. The continuum model results assume an effective crack tip radius of $\rho = 2.0 \text{ \AA}$. The continuum predictions confirm the strengthening effects of the QM-CADD simulations, albeit at a smaller magnitude.

Impurity type	Bader charge		QM-CADD		Continuum	
	Impurity	Nearest Al	K_{IN}	Impurity effect	K_{IN}	Impurity effect
Pure Al		-0.02	0.245		0.246	
Hydrogen	-1.27	1.36	0.310	27%	0.265	7.8%
Oxygen	-2.11	2.26	0.300	22%	0.265	7.8%
Chlorine	-1.20	1.07			0.258	5.0%
Fluorine	-1.23	1.20			0.259	5.4%
Sodium	1.00	0.42			0.248	0.8%
Lithium	1.00	-0.87			0.245	-0.4%

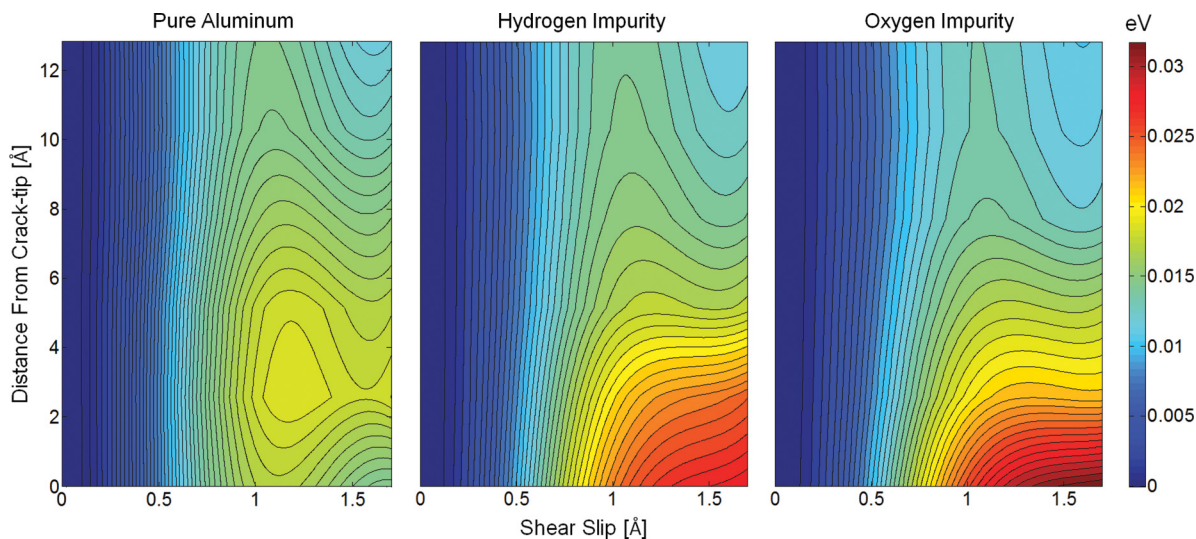


FIG. 4. (Color online) Contour plots for the calculated stacking fault energy surfaces are shown for the pure aluminum, hydrogen, and oxygen configurations (from left to right, respectively). The energy vs slip relationship shows a trend of convergence toward the theoretical bulk stacking fault energy curve with increasing distance from the crack tip. The presence of the free surface clearly raises the stacking fault energy to a depth of 1 nm into the material, and both impurity atoms produce an even larger increase in energy within the first few atomic layers.

nucleation from an aluminum crack tip involves a dislocation very close the surface (~ 1 nm),²¹ substantial inaccuracies can result if the bulk stacking fault energies are used in the model. This finding justifies the approach taken here.

Despite its simplifying assumptions, the Peierls continuum model predicts that both hydrogen and oxygen inhibit crack tip plasticity, in agreement with the QM-CADD simulations (Table I). Given the continuum model's success at reproducing the QM-CADD simulation results, it was used to examine the effect of four additional impurity elements. Considering that chlorine, fluorine, lithium, and sodium relax to a similar location at the crack tip, the prediction of their impact on nucleation was amenable to the continuum model. While fluorine and chlorine both exhibited a strengthening effect, neither impurity is predicted to have as strong of an effect as oxygen and hydrogen. In contrast, sodium and lithium each had a negligible effect on the critical nucleation load, both creating less than a 1% change in the critical load relative to pure aluminum. Loosely speaking, these results are consistent with the general understanding that surface impurities affect the bond strength on the slip plane through localized charge transfer. While the addition of electropositive atoms such as lithium and sodium produced negligible perturbations in the charge density field of the crack tip, the other electronegative impurities had a much larger effect.

Focusing on a bare aluminum crack tip in the presence of surface impurities, our findings are most pertinent to the effort to illuminate the mechanisms through which the environment can influence near threshold fatigue crack growth. Experimentally, as the partial pressure of reactive impurity agents is increased or the frequency of fatigue loading decreased (promoting transport to the crack tip), the rate of crack growth per loading cycle is generally found to increase, consistent with an environmental embrittling effect.^{2,22} Noting the absence of a surface oxide film in this work, the environmental effects

observed here would correspond to experimental fatigue crack growth in a very strong, but not perfect, vacuum environment.

Recent dislocation dynamics simulations clearly show that the rate of fatigue crack growth depends both on the behavior of dislocations in the bulk of the material near the crack tip and the local energy required to propagate the crack tip forward.²³ We note that the latter depends not only the energy required to decohere atomic planes, but also on the energy associated with crack tip dislocation nucleation prior to propagation.²⁴ While it is possible that preexisting dislocations will dominate crack tip blunting in a ductile material such as aluminum, it is clear that some form of incremental competition between crack advancement and dislocation nucleation must play a role in determining the near threshold fatigue strength. The literature suggests that both of these mechanisms may be influenced by the environment, particularly by atomized hydrogen impurities.^{1,3,4}

At the crack tip, embrittlement is often attributed to impurities weakening interatomic bonding, and therefore enhancing decohesion^{6,27,28} and/or crack tip dislocation nucleation.²⁹ At first sight, the *ab initio* predictions made here are in direct contrast to the idea that impurity elements such as hydrogen should enhance dislocation nucleation at the crack tip. However, further consideration is warranted, in that it is possible that the presence of impurities may encourage dislocations to form on the slip plane directly in front of the crack tip, as observed here in the case of hydrogen (Fig. 2). In this case, dislocation nucleation will lead to incremental decohesion.

The idea that the presence of impurities at the crack tip lowers the cohesive energy is another mechanism that may lead to embrittlement. This mechanism is consistent with *ab initio* predictions that show that the presence of hydrogen on a potential crack plane in bulk aluminum lower the cohesive energy of that plane.⁶ Here we examined the role of surface

hydrogen on the cohesive energy of the crack plane which activated in the QM-CADD simulation with hydrogen. For the configuration examined here, the cohesive energy was not found to be influenced by the presence of hydrogen on the surface of the crack. Thus, the crack tip hydrogen embrittlement observed in our QM-CADD simulation can be attributed solely to hydrogen inhibiting dislocation nucleation. Overall, it is important to recognize that the findings of this work are likely sensitive to the specific atomic configuration of the crack tip and impurity elements that were studied, noting that the impurity elements were placed in the surface location, where we suspect they would most strongly influence dislocation nucleation.

In summary, we have performed three direct quantum-mechanical multiscale simulations of a loaded crack tip, predicting that hydrogen and oxygen surface impurities inhibit the onset of plasticity. While the addition of oxygen allowed the onset of plasticity to occur on the same slip plane as the pure aluminum configuration, the addition of hydrogen

forced plasticity to occur on an alternate slip plane, leading to incremental crack growth. In order to obtain more insight into the inhibition of plasticity by surface impurity elements, we have employed a quantum-mechanically informed continuum model to predict the critical load at which a dislocation will nucleate from the crack tip. The continuum model confirmed the impurity strengthening mechanism found in the multiscale model, thus more firmly establishing that plasticity can be inhibited by surface impurities. When compared to other work with bulk impurities, it is clear that the strengthening mechanism observed here is dependent on the geometry of the surface and the depth of adsorption. These factors motivate further investigation into the nature of environment assisted fatigue.

This primary support for this research was provided by Paul Hess at ONR (Grant No. N000141010323). Additional support was provided by Ed Glaessgen at NASA (Grant No. NNX08BA39A), Ali Sayir at AFOSR (FA95501110273), and the NSF IGERT Program (Grant No. DGE-0903653).

-
- ¹S. P. Lynch, in *Gaseous Hydrogen Embrittlement of Materials in Energy Technologies*, edited by R. Gangloff and B. Somerday (Woodhead, Cambridge, 2012).
- ²S. E. Stanzl, H. R. Mayer, and E. K. Tscheegg, *Mater. Sci. Eng., A* **147**, 45 (1991).
- ³S. P. Lynch, *Metallography* **23**, 147 (1989).
- ⁴Y. Liang, P. Sofronis, and N. Aravas, *Acta Mater.* **51**, 2717 (2003).
- ⁵J. Song, M. Soare, and W. A. Curtin, *Modell. Simul. Mater. Sci. Eng.* **18**, 045003 (2010).
- ⁶D. E. Jiang and E. A. Carter, *Acta Mater.* **52**, 4801 (2004).
- ⁷S. Aubry, K. Kang, S. Ryu, and W. Cai, *Scr. Mater.* **64**, 1043 (2011).
- ⁸G. Lu, D. Orlikowski, I. Park, O. Politano, and E. Kaxiras, *Phys. Rev. B* **65**, 064102 (2002).
- ⁹N. Bernstein, J. R. Kermode, and G. Csanyi, *Rep. Prog. Phys.* **72**, 026501 (2009).
- ¹⁰S. A. Serebrinsky, E. A. Carter, and M. Ortiz, *J. Mech. Phys. Solids* **52**, 2403 (2004).
- ¹¹S. Ogata, F. Shimojo, R. K. Kalia, A. Nakano, and P. Vashishta, *J. Appl. Phys.* **95**, 5316 (2004).
- ¹²A. K. Nair, D. H. Warner, and R. G. Hennig, *J. Mech. Phys. Solids* **59**, 2476 (2011).
- ¹³A. K. Nair, D. H. Warner, R. G. Hennig, and W. A. Curtin, *Scr. Mater.* **63**, 1212 (2010).
- ¹⁴L. E. Shilkrot, R. E. Miller, and W. A. Curtin, *Phys. Rev. Lett.* **89**, 025501 (2002).
- ¹⁵G. Kresse and J. Hafner, *Phys. Rev. B* **48**, 13115 (1993).
- ¹⁶G. Kresse and J. Hafner, *J. Phys.: Condens. Matter* **6**, 8245 (1994).
- ¹⁷M. Methfessel and A. T. Paxton, *Phys. Rev. B* **40**, 3616 (1989).
- ¹⁸K. Momma, and F. Izumi, *J. Appl. Crystallogr.* **41**, 653 (2008).
- ¹⁹W. Tang, E. Sanville, and G. Henkelman, *J. Phys.: Condens. Matter* **21**, 084204 (2009).
- ²⁰J. R. Rice, *J. Mech. Phys. Solids* **40**, 239 (1992).
- ²¹D. H. Warner, W. A. Curtin, and S. Qu, *Nat. Mater.* **6**, 876 (2007).
- ²²P. S. Pao, M. Gao, and R. P. Wei, *Scripta Metall.* **19**, 265 (1985).
- ²³V. S. Deshpande, A. Needleman, and E. Van der Giessen, *Acta Mater.* **50**, 831 (2002).
- ²⁴D. Farkas, M. Duranduru, W. A. Curtin, and C. Ribbens, *Philos. Mag. A* **81**, 1241 (2001).
- ²⁵E. B. Tadmor and S. Hai, *J. Mech. Phys. Solids* **51**, 765 (2003).
- ²⁶M. Creager and P. C. Paris, *Int. J. Fract.* **3**, 247 (1967).
- ²⁷A. R. Troiano, *Trans. ASM.* **52**, 54 (1960).
- ²⁸R. A. Oriani, *Ber. Bunsenges. Phys. Chem.* **76**, 848 (1972).
- ²⁹S. P. Lynch, *Acta Metall. Mater.* **36**, 2639 (1988).